16

TID-23650

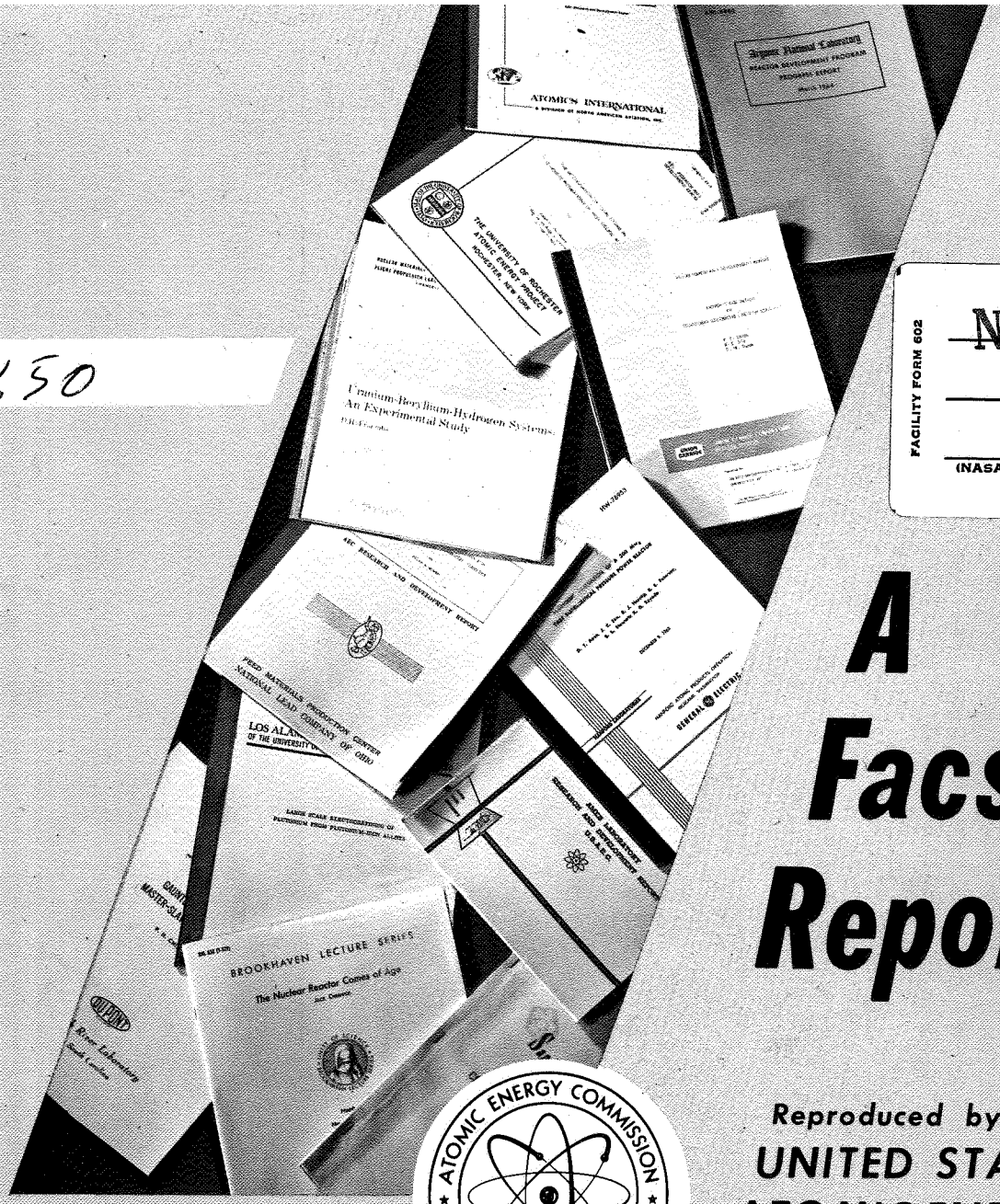

A Facsimile Report

Reproduced by
UNITED STATES
ATOMIC ENERGY COMMISSION
Division of Technical Information
P.O. Box 62 Oak Ridge, Tennessee 37830

SP50194K

AEROJET GENERAL TIRE GENERAL

REPORT NO. RN-S-0168
TO
AEC-NASA SPACE NUCLEAR PROPULSION OFFICE

NES EXHAUST PLUME SCALE-MODEL MEASUREMENTS AND FULL-SCALE PREDICTIONS

NERVA PROGRAM

CONTRACT SNP-1 NOVEMBER 1964

AEROJET-GENERAL CORPORATION
A SUBSIDIARY OF THE GENERAL TIRE & RUBBER COMPANY

ABSTRACT

This report presents the predicted full-scale NES exhaust plume length and exhaust plume thermal radiation flux at proximate surfaces, and the methods used to predict full-scale flame length and thermal radiation from scale-model data. Also presented are experimental values of scale-model NES exhaust-plume length, exhaust-plume thermal radiation flux at proximate surfaces, and exhaust-plume emittance.

W. D. Stinnett
REON Technical Systems Manager

CONTENTS

	Page
I. INTRODUCTION	1
II. FULL-SCALE EXHAUST PLUME PREDICTIONS	1
III. DISCUSSION	2
A. Exhaust-Plume Shape	2
B. Exhaust-Plume Thermal Radiation to Proximate Surfaces	4
C. Exhaust-Plume Emittance Measurements	6
D. Exhaust-Plume Flame Temperature	7
E. Full-Scale Thermal Radiation	9
References	12
Symbols	13

	Figure
Predicted Hydrogen Exhaust Plume Size and Shape	1
Predicted Thermal Radiation Flux Q(Btu/ft^2-sec) from Full Scale NERVA Exhaust Plume at Selected Locations	2
Temperature Rise for Thick Concrete Slab as a Function of Time ($\Delta\Theta$) and Distance from Slab Surface (X) for Radiative Heat Fluxes Q = 5.0, 10.0 and 20.0 Btu/ft^2-sec	3
Temperature Rise (ΔT) for 14-Gage (0.064) Sheet Aluminum Receiving a Constant Radiative Heat Flux of 5 Btu/ft^2-sec as a Function of Time ($\Delta\Theta$) and Adjacent Air Convection Coefficient (h_c)	4
Temperature Rise (ΔT) for 14-Gage (0.064) Sheet Aluminum Receiving a Constant Radiative Heat Flux of 10 Btu/ft^2-sec as a Function of Time ($\Delta\Theta$) and Adjacent Air Convection Coefficient (h_c)	5
Temperature Rise (ΔT) for 14-Gage (0.064) Sheet Aluminum Receiving a Constant Radiative Heat Flux of 20 Btu/ft^2-sec as a Function of Time ($\Delta\Theta$) and Adjacent Air Convection Coefficient (h_c)	6

CONTENTS (cont.)

	Figure
Exhaust Plume From 1/4-Scale Nuclear Exhaust System (SST-2) Test No. D-280-LQ-35 (Night Firing)	7
Thermal Radiation Flux Q (Btu/ft^2-sec) From 1/8-Scale NERVA Exhaust Plume at Selected Locations	8
Thermal Radiation Flux Q (Btu/ft^2-sec) From 1/4-Scale NERVA Exhaust Plume at Selected Locations	9
Diagram and Calibration Curve for Radiometer Used to Measure Exhaust Plume Emittance	10
Measured Values of 1/4-Scale Exhaust Plume Thermal Emittance as a Function of Position Along Plume Centerline	11

I. INTRODUCTION

This report presents discussions of the methods used to predict the length of the full-scale NES exhaust plume and exhaust-plume thermal radiation to proximate surfaces.

During 1/8- and 1/4-scale model testing of the NERVA Exhaust System, measurements were made of exhaust-plume length, exhaust-plume thermal radiation to proximate surfaces, and exhaust-plume thermal emittance. The expected length of full-scale NES exhaust plume and expected exhaust-plume thermal radiation to proximate surfaces were determined by analysis, using these scale-model measurements.

II. FULL-SCALE EXHAUST PLUME PREDICTIONS

The predicted exhaust-plume size and shape, based on both test data and analysis, is illustrated in Figure 1; the predicted thermal radiation from the exhaust plume to proximate surfaces is illustrated in Figure 2.

The accuracy of the predicted flame length is estimated to be +20% and -0%; that is, the flame could be up to 20% longer but it is not expected to be any shorter in length.

It is estimated that the full-scale thermal radiation from the exhaust plume will not be much higher (within 10%) than the higher values presented in Figure 2, but it is possible that the radiation flux could be much lower (possibly 50%) than the values presented in Figure 2.

Temperature rise-time data were calculated for the concrete drainage ditch floor and walls (Figure 3), and the aluminum radiation shields (Figures 4, 5, and 6). Temperature rise-time information can be obtained for various locations by using the data presented in Figures 3, 4, 5, and 6 in conjunction with the predicted local thermal radiation flux presented in Figure 2.

It is recommended that calorimeters and/or radiometers be used to measure the local thermal-radiation flux during the preliminary tests (ambient hydrogen and low-power) at ETS-1. It is recommended that calorimeters be positioned: (1) on the south drainage/ditch wall (near top of the wall and about 90 ft below duct exit); (2) on the vault door (5 D_s* above and 10 D_s to the side of the duct exit); and (3) on the superstructure above the concrete vault (in line with centerline of duct and 30 to 60 ft above vault roof). Data obtained from these preliminary tests will serve as a check in predicting the thermal radiation flux during full power tests.

III. DISCUSSION

A. EXHAUST-PLUME SHAPE

Part of the analysis to determine the thermal radiation from the hydrogen exhaust flame is to establish a model to predict the flame shape. Hawthorne, Waddell, and Hottel (Reference 1) have developed a model in which flame length is derived by applying the laws of conservation of mass and momentum, and an equation of state, along with the assumption that the flame shape is an inverted right circular cone (i.e., the angle spread of the flame is a constant). Their equation for flame length is

$$L_f/D_e = \frac{k_f}{C_t}\sqrt{\frac{\overline{T}_f}{\alpha\, T_e}\left[C_t + (1-C_t)\,\frac{M_s}{M_e}\right]} \qquad (1)$$

(The meanings of symbols are presented at the end of the text of this report).

Equation (1) takes into account the effects of density, temperature, and chemical reaction, but neglects the effect of buoyancy. The Froude number (N_{FR}), which is a measure of suppression of buoyancy effects upon flame burning characteristics was found to be extremely high in the scale-model system. Therefore, buoyancy should have only a small effect on increasing the burning rate and on decreasing the flame length in the exhaust plume. The Froude number is given by the expression

*D_s = 4.33 ft = internal diameter of duct exit.

$$N_{FR} = \mu_e^2/g\,D_e \qquad (2)$$

where μ_e equals duct-exit velocity, g equals gravitational constant, and D_e equals duct-exit diameter. The Froude numbers for the 1/8-scale model system were on the order of 2×10^6, for the 1/4 scale model system were on the order of 0.5×10^6, and will be about 0.6×10^6 for the full scale system.

The constant k_f in Equation (1) is, to a degree, a function of the Froude number. Hawthorne, Waddell, and Hottel (Reference 1) used an average value for k_f ($k_f = 5.3$) in their expression for flame length of free turbulent exhaust flames, but indicated that k_f generally increases with increasing Froude number.

An estimate of flame length was made from motion pictures and still photos taken from the hydrogen flame from the eighth and quarter scale model systems. Eighth scale test measurements from movies and still photos indicate a flame length of 85 and 75 duct-exit diameters, respectively. Equation (4)* of REON Report 2678 predicts a flame length of 93.7 duct exit diameters for the conditions under which the test was conducted. Quarter-scale test measurements of still photographs taken during a night test indicate a visible flame length of approximately 70 to 75 duct exit diameters (Test D-280-LQ-35; see Figure 7). Equation (1) predicts a theoretical flame length of 56 duct-exit diameters for the conditions under which the test was conducted.

For the full-scale system and the expected testing conditions, Equation (1) predicts a theoretical flame length of approximately 40 exit diameters. This theoretical length of 40 exit diameters is based on the assumption that the full scale flame spread angle is the same as the quarter scale flame spread angle. Based on the quarter scale visible flame length and the ratio of theoretical full-scale flame length to theoretical 1/4-scale flame length, a full-scale visible flame length of 53.6 exit diameters is indicated. Figure 1 shows a sketch illustrating the expected dimensions of the full-scale exhaust plume shape.

*Equation (4) of REON Report 2678 is identical with Equation (1) of the present report, except that the equation in the earlier report lacks the α term which appears as an $(\alpha)^{-0.5}$ factor in Equation (1) of this report. (Note: $\alpha = 1.5$).

Quarter-scale still photographs indicate that the hydrogen-air flame is considerably larger in size when the secondary flow rate is zero. Photographic measurements indicate that the addition of nitrogen reduces the exhaust plume size by 15 to 20% (analytical results predict a similar reduction). It is expected that the full-scale secondary fluid steam will have essentially the same effect as nitrogen.

B. EXHAUST-PLUME THERMAL RADIATION TO PROXIMATE SURFACES

The exhaust plume, a high-temperature gas mixture containing superheated steam, is a source of thermal radiation. It is important to determine the magnitude of this thermal radiation in order to ascertain the thermal environment of the exhaust duct and that of any hardware and structure associated with the operation.

A calorimeter* and radiometer manufactured and calibrated by Hy-Cal Engineering, Santa Fe Springs, California, was used to measure the thermal radiation at various locations in the vicinity of the exhaust plume from both the 1/8- and 1/4-scale systems. These measurements are presented in Figures 8 and 9, respectively. The 1/4-scale test model included the secondary duct drain pipe below the exit of the duct. A small air-hydrogen flame exits near the exit of the drain pipe and contributes significant thermal radiation to nearby surfaces. The 1/4-scale duct system did not include the drainpipe.

1. Concrete Surfaces

A concrete surface is an excellent absorber of thermal radiation because of its high surface emissivity. The surface emissivity of concrete surfaces ranges from 0.8 to 0.9. The surfaces nearer to the exhaust plume and the drainpipe exhaust plume will be subject to extremely high thermal loads. Figure 3 shows the temperature rise in a thick concrete slab as a function of time and thermal radiation flux. Figure 3 indicates higher than the actual temperature rise because the effects of local convective cooling and re-radiation to local objects and atmosphere were neglected. Nevertheless,

*The calorimeter was damaged beyond repair after a few 1/8-scale tests and, therefore, did not produce much data.

the true temperatures are expected to be extremely high at certain points on the concrete surface (i.e., on the order of 1000 to 2000°F) and it is expected that the surface of the concrete, if not cooled, will spall and flake because of high temperatures and high temperature gradients. High temperature will break down the cement-water matrix, causing the concrete to lose its strength; it will also cause gases to force their way out of the concrete, producing what is known as "popping." The large temperature gradient will introduce high local thermal stresses, which will contribute to the surface damage.

One way to prevent damage to the concrete surface would be to cool it with the duct coolant water. It would be possible to divert some of the coolant water coming out of the duct cooling discharge pipe and distribute it over the hotter portions of the concrete floor in the drainage ditch.

2. Effects of Exhaust-Plume Thermal Radiation on Radiation Shields

Protective radiation shields made of 0.064-in.-thick aluminum sheets have been placed on the exterior of the vault door and vault superstructure to reflect thermal radiation received from the exhaust plume. It is estimated that the vault door will experience incident thermal radiation fluxes from 10 to 28 Btu/ft^2-sec.

Figures 4, 5, and 6 show the temperature increase as a function of time and local convection coefficient for 14-gage (0.064-in.) aluminum sheet receiving constant thermal radiation fluxes of 5, 10, and 20 Btu/ft^2-sec, respectively. For these figures, it was assumed that the normal surface emissivity of the aluminum is equal to 0.056, and that internal thermal resistance of the sheet is negligible. These figures show that the local convection coefficient highly influences the temperature rise. The magnitude of the local convection coefficient will be influenced by both natural convection and forced convection. The natural convection is caused by buoyancy forces acting on the hot air adjacent to the aluminum sheet; and the forced convection is caused by local air currents introduced by the presence of the exhaust plume. It is not known how the effects of natural and forced convection will interact to give a resultant local convection coefficient, but study indicates that the average local convection coefficient on the radiation shields will be between 2 and 5 Btu/hour-ft^2-°F.

After a test, the full-scale radiation shields should be inspected for damage and/or oxidation effects. Any surfaces that become oxidized should be cleaned or replaced with new aluminum sheets. Oxidation can cause the surface emissivity to increase by approximately 150%; such an increase would most probably cause the hottest parts of the radiation shield to melt during the following test.

3. Variation in Radiation to Proximate Surfaces

Large variations in incident thermal radiation have been measured at the same location from test to test under approximately equal testing conditions. The cause or causes for these variations, which are as great as a 100% increase in measured radiation, is not known. The variations could be partially caused by errors in data acquisition or changes in the radiometer calibration. They could also be caused by wind conditions. Changes of this sort have been reported, by LASL during KIWI and NASA-Lewis tests, in which the wind changed direction and the measured value of thermal radiation doubled in value.

4. Miscellaneous Test Equipment

Any test equipment or any other material within 100 yards of the exhaust plume, and in a direct sight-line to the plume, should be shielded. Such items as equipment, wire, wood objects, rubber, etc., should be covered with a protective thermal radiation shield of aluminum sheet or foil.

C. EXHAUST-PLUME EMITTANCE MEASUREMENTS

A radiometer was constructed and calibrated to measure the exhaust plume emittance and measurements were made from the 1/4-scale test model. Emittance measurements are necessary for developing a model for predicting thermal radiation from the plume to proximate surfaces. A schematic, calibration data, and other pertinent details of the radiometer are presented in Figure 10. Emittance measurements were obtained at various positions along the flame length; during these measurements the radiometer was sighted at the

flame centerline in such a way that the centerline axis of the radiometer made a right angle with respect to the flame centerline. The 1/4-scale exhaust plume emittance data are presented in Figure 11. Poor alignment in sighting the radiometer at the exhaust plume and local wind conditions are probably responsible for scatter among these data.

It was discovered in quarter scale tests D-280-LQ-35 and -36 that the addition of the secondary fluid nitrogen reduced the emittance by 20 to 25%. This was verified by thermal radiation measurements at a proximate surface. During the first part of tests -35 and -36 only, the primary fluid was flowed at design and approximately half-design values, respectively. Secondary fluid (N_2) was introduced after the primary fluid had flown at the prescribed flow rates for a few seconds. In addition to reducing the emittance, the plume size was also reduced. During full-scale testing, the secondary fluid will be steam. It is estimated that the addition of steam to a hydrogen-air flame will have essentially the same effect in reducing the flame or plume size but, since steam is a good radiator and nitrogen is a poor radiator, steam addition will not reduce the flame thermal emittance as much as the addition of nitrogen.

D. EXHAUST-PLUME FLAME TEMPERATURE

Two methods were used to measure the gas temperature in the exhaust plume during 1/8- and 1/4-scale model tests; the methods were: the positioning of thermocouples in the exhaust plume, and measurement of flame emittance with a radiometer, followed by use of emittance values to estimate flame temperature.

During 1/8-scale testing, a chromel-alumel thermocouple was placed in the exhaust plume but the combined effects of temperature and velocity damaged the thermocouple and no data was obtained. During 1/4-scale testing, chromel-alumel thermocouples were placed in the approximate center of the drainpipe flame. Temperatures as high as slightly more than 2500°R were recorded. The sum of the conduction and radiation temperature losses for these thermocouples would be quite high, probably at least 500°R. Thus, a minimum temperature of at least 3000°R was indicated.

During 1/8-scale, testing an approximate flame temperature of 2700°R was estimated from a lead sulfide radiometer measurement. Further study indicates this temperature of 2700°R was a low estimate and that a better estimate would have been approximately 3200 to 3400°R. Emittance measurements during 1/4-scale testing also indicate a flame temperature of at least 3200 to 3400°R. Temperatures obtained during scale testing from emittance measurements are based on the flame thickness (obtained from photographs taken during a night test), and estimates (estimated from a conservative viewpoint) of the partial pressure of the steam, the principal emitting species, in the flame at the location of emittance measurement.

Based on the above considerations, it is estimated that average scale model flame temperature was approximately 3300°R. The flame temperature for the 1/8- and 1/4-scale tests should have been essentially the same because the pre-combustion mixture temperature and mixture ratio were essentially the same during 1/8- and 1/4-scale tests.

It should be mentioned that the flame (exhaust-plume) is highly turbulent and the many local burning fronts in the flame have a wide variety of compositions (hydrogen to air and N_2/steam ratio). This will cause the flame to contain many different local temperatures: some above average and some below average.

Figure 5 in Reference 2 was used as a guide for estimating the full scale flame temperature. Study of Figure 5, Reference 2, and using the expected full scale pre-combustion mixture temperature (assuming the average full-scale pre-combustion mixture is approximately the same as scale model mixture) indicates an average full scale flame temperature of approximately 4600°R.

Study of Figures 5, 14, and 15 of Reference 2 and analysis indicated the lower limit scale-model temperature of approximately 2700°R, and a corresponding lower limit full-scale flame temperature of approximately 4200°R.

This estimated average full-scale flame temperature of 4600°R is probably higher than the actual average full-scale flame temperature. The

temperature 4600°R is based on the assumption that the pre-combustion mixture ratio of H_2, secondary fluid (H_2O for full-scale conditions), and air are the same during full-scale test conditions as during scale-model test conditions. Actually, during the full-scale test conditions, the much higher pre-combustion mixture temperature will shift the flammability limits in such a way that less air is required to initiate and sustain combustion; this effect, other things being equal, will produce a cooler flame. Actually, this effect will be slightly offset by the fact that H_2O will be used under full-scale test conditions, while N_2 was used under scale-model test conditions. Addition of H_2O (Reference 2, page 13) has more effect on the flammability limits than N_2; that is, more air is required and, consequently, a hotter flame, to initiate combustion when H_2O is added than when N_2 is added.*

Based on the above reasoning, it is estimated that 4600°R is the upper limit for the average flame temperature during full-scale test conditions.

The ratio of full-scale flame temperature to scale-model flame temperature, based on the experiment and analysis, is then roughly

$$1.35 \text{ to } 1.44 \left(\text{where } \frac{4600}{3400} = 1.35 \text{ and } \frac{4600}{3200} = 1.44\right)$$

E. FULL-SCALE THERMAL RADIATION

The full-scale exhaust-plume emittance and, consequently, the thermal radiation to proximate surfaces, will be considerably greater than scale-model exhaust plume emittance and radiation to proximate surfaces. The primary reason is that the full-scale flame (or exhaust plume) temperature ($T_{f_{FS}}$) will be much greater than the flame temperature ($T_{f_{SM}}$) of the scaled models. The effective emissivity of the flame also influences the emittance, but analysis indicates that the full-scale flame emissivity (ϵ_{FS}) will not differ greatly from the scale model emissivity (ϵ_{SM}) and, therefore, flame emissivity will have only a secondary effect upon flame emittance.

*Actually, this phenomena could be partially offset because H_2O (steam) has a higher specific heat than N_2 and, thus, H_2O would cool the flame more than N_2.

1. Determination of Full Scale Emittance (W_{FS})

The local full-scale flame emittance (W_{FS}) is related to local scale model emittance (W_{SM}) by the expression

$$W_{FS}/W_{SM} = \left(\epsilon_{FS}/\epsilon_{SM}\right)\left(T_{f_{FS}}/T_{f_{SM}}\right)^4 \qquad (3)$$

It was estimated that the ratio $\left(T_{f_{FS}}/T_{f_{SM}}\right)$ is approximately 1.35 to 1.44 (see Section III,4). This estimate is based on scale-model exhaust plume temperature measurements, known scale-model and full-scale temperatures of hydrogen and secondary fluid mixture prior to combustion, basic thermodynamics, and an estimated full-scale flame temperature based on a careful study (both a quantitative and qualitative basis) of Figures 5, 14, and 15 in Reference 2.

Penner and Thompson (Reference 3) show that emissivity of water vapor is a function of the temperature and optical density, where optical density is the product of the partial pressure of the radiating species (H_2O) and the thickness of the gas cloud* containing the radiating species. Study of Figure 7 in Reference 3 shows that, other factors being equal, emissivity decreases with increasing flame temperature, and increases with increasing thickness of the gas cloud. Based on the ratio $\left(T_{f_{FS}}/T_{f_{SM}}\right) = 1.35$ to 1.44, the fact that the full scale exhaust plume dimensions will be approximately four times the quarter scale dimensions, and neglecting the increase in partial pressure of the radiating cloud species (H_2O) because of full-scale secondary steam injection, Figure 7 of Reference 3 indicates that $\left(\epsilon_{FS}/\epsilon_{SM}\right)$ is approximately equal to one. During full scale operations it is estimated that the secondary injection of steam by the gas generator into the primary hydrogen fluid will cause the average emissivity to increase by less than 10%; therefore, it will be assumed that $\left(\epsilon_{FS}/\epsilon_{SM}\right) = 1.10$.

*Cloud is analogous to exhaust plume or exhaust flame.

Using the upper limit $T_{f_{FS}} / T_{f_{SM}} = 1.44$ and $\epsilon_{FS}/\epsilon_{SM} = 1.10$, Equation (3) gives $\frac{W_{FS}}{W_{SM}} = (1.10)(1.44)^4 = 4.72$. Thus, a correction factor $C_f = W_{FS}/W_{SM} = 4.72$ will be used to convert scale model emittance to full scale emittance.

This correction factor C_f was also used to convert small-model incident radiation on proximate surfaces to full-scale incident radiation. This approximation is conservative in that analysis (Reference 1) shows that the full-scale plume dimensions in terms of duct exit diameters should decrease with respect to scale model plume dimensions.

The expected maximum full-scale thermal radiation fluxes for various locations are presented in Figure 2.

It was estimated that first, the thermal radiation flux incident on the vault superstructure radiation shields will be approximately 10 Btu/ft^2-sec, and, second, the thermal radiation flux incident upon the drainage ditch walls will be approximately 10 to 15 Btu/ft^2-sec.

REFERENCES

1. W. R. Hawthorne, D. S. Waddell, and H. C. Hottel, "Mixing and Combustion in Turbulent Gas Jets," Third Symposium on Combustion, Flame and Explosion Phenomena, pp. 266 to 280, Williams and Wilkins, Baltimore, 1949.

2. I. S. Drell and F. E. Belles, Survey of Hydrogen Combustion Properties, NACA Report 1383, 1958.

3. S. S. Penner and A. Thompson, "Determination of Equilibrium Infrared Gas Emissivities from Spectroscopic Data," Transport Properties in Gases, Proceedings of Second Biennial Gas Dynamics Symposium, August 1957, Evanston, Illinois, Figure 7, p. 171.

SYMBOLS

C_t = Mol fraction of duct fluid in the unreacted stoichiometric mixture

D_e = Nozzle or duct exit diameter

k_f = Constant defining the angle spread of the flame ($k_f = \frac{1}{\tan \beta}$ = cotangent β, where β is the angle between the flame centerline and a line of the flame surface - assuming the plume has the shape of an inverted right circular cone)

L_f = Visible flame length

M_s = Molecular weight of fluid surrounding plume

M_e = Molecular weight of duct fluid in duct exit plane

$\bar{T}_f$ = Adiabatic stoichiometric flame temperature, absolute

T_e = Absolute temperature of duct fluid at duct exit

T_f = Flame temperature

$T_{f_{FS}}$ = Flame temperature, full-scale

$T_{f_{SM}}$ = Flame temperature, scale-model

W = Emittance

W_{FS} = Emittance, full-scale

W_{SM} = Emittance, scale-model

α = Mols of reactants per mols of products, for the stoichiometric mixture

ϵ_{FS} = Emissivity, full-scale

ϵ_{SM} = Emissivity, scale-model

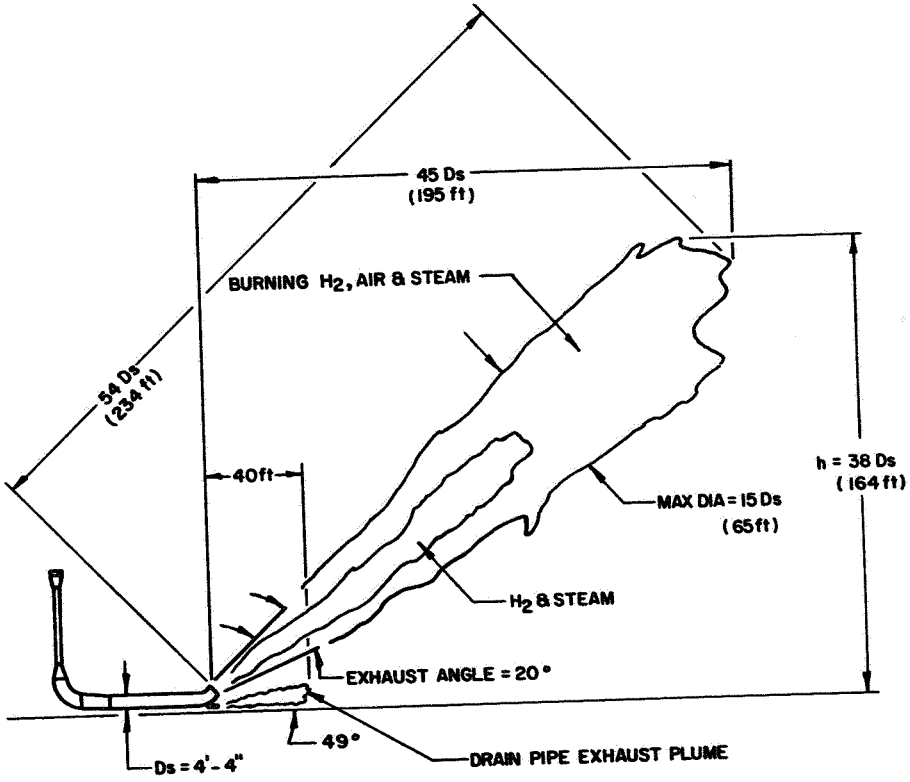

Predicted Hydrogen Exhaust Plume Size and Shape

Figure 1

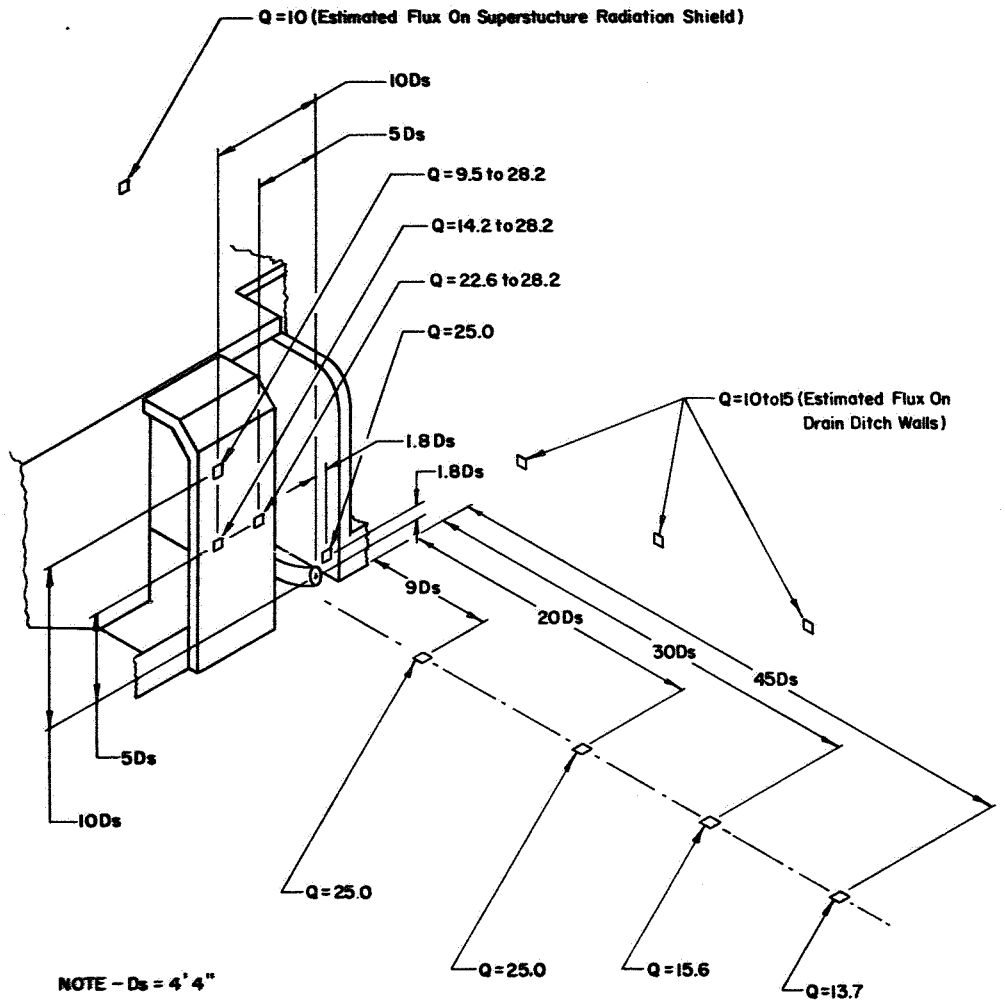

Predicted Maximum Thermal Radiation Flux (Q, Btu/ft^{2}sec)
From Full-Scale NERVA Exhaust Plume
at Selected Locations

Figure 2

NOTES. 1. ASSUMED PROPERTIES OF CONCRETE:
k_c = THERMAL CONDUCTIVITY = 0.75 Btu/ft·°F·hr
α_c = THERMAL DIFFUSIVITY = 0.704 x 10^{-5} ft^2/sec
ϵ_c = SURFACE EMISSIVITY = 0.88
2. NO CONVECTION COOLING OF SLAB SURFACES
3. LEGEND

SYMBOL	Q (Btu/ft^2 sec)
———	20.0
—·—·—	10.0
- - - - - -	5.0

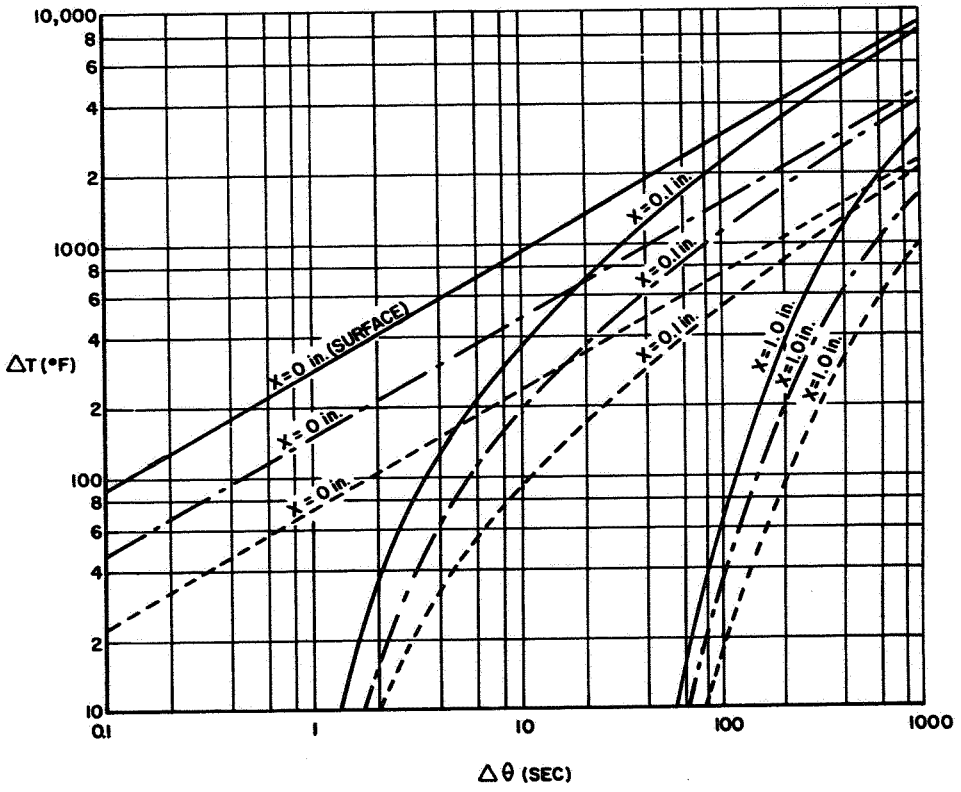

Temperature Rise for Thick Concrete Slab as a Function of
Time ($\Delta\theta$) and Distance From Slab Surface (X) for
Radiative Heat Fluxes, Q = 5.0, 10.0, and 20.0 Btu/ft^{2}sec

Figure 3

ASSUMPTIONS

1. SURFACE EMISSIVITY (ϵ) = 0.056
2. NO THERMAL GRADIENT THROUGH SHEET
3. AIR AMBIENT TEMPERATURE = CONSTANT

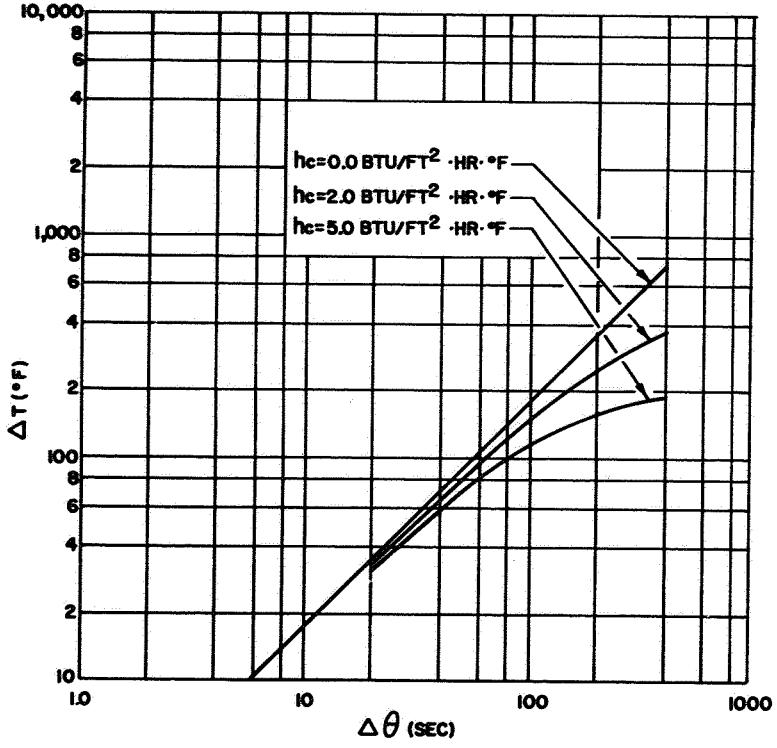

Temperature Rise (ΔT) for 14-Gage (0.064) Sheet Aluminum Receiving a Constant Radiative Heat Flux of 5 Btu/ft^{2}sec as a Function of Time ($\Delta\theta$) and Adjacent Air Convection Coefficient (h_c)

Figure 4

RN-S-0168

ASSUMPTIONS.

1. SURFACE EMISSIVITY(ϵ) = 0.056
2. NO THERMAL GRADIENT THROUGH SHEET
3. AIR AMBIENT TEMPERATURE = CONSTANT

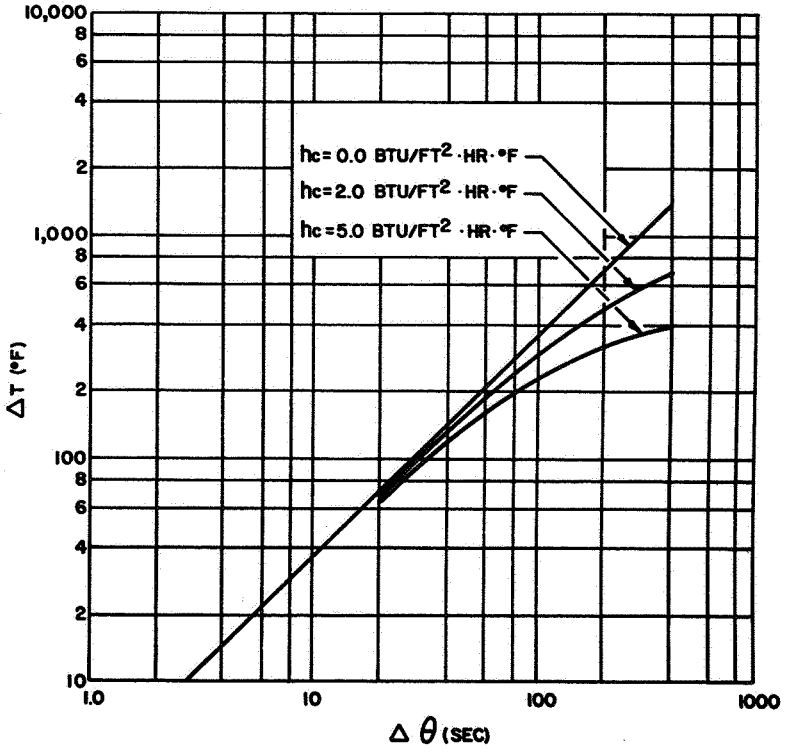

Temperature Rise (ΔT) for 14-Gage (0.064) Sheet Aluminum Receiving a Constant Radiative Heat Flux of 10 Btu/ft^{2}sec as a Function of Time ($\Delta\theta$) and Adjacent Air Convection Coefficient (h_c)

Figure 5

ASSUMPTIONS

1. SURFACE EMISSIVITY (ϵ) = 0.056
2. NO THERMAL GRADIENT THROUGH SHEET
3. AIR AMBIENT TEMPERATURE = CONSTANT

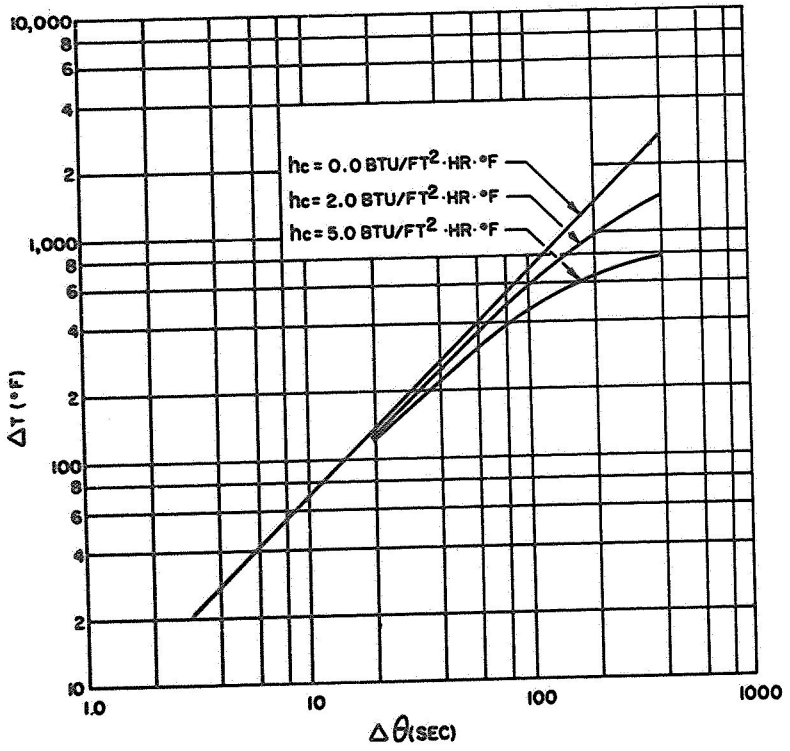

Temperature Rise (ΔT) for 14-Gage (0.064) Sheet Aluminum Receiving a Constant Radiative Heat Flux of 20 Btu/ft^{2}sec as a Function of Time ($\Delta\theta$) and Adjecent Air Convection Coefficient (h_c)

Figure 6

RN-S-0168

Exhaust Plume From 1/4-Scale Nuclear Exhaust System (SST-2)
Test No. D-280-LQ-35 (Night Firing)

Figure 7

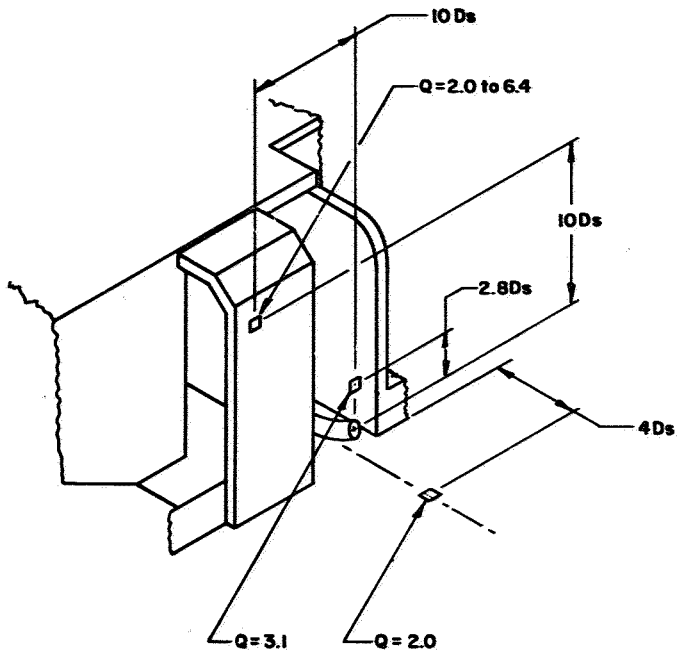

NOTE — Ds = 6.4"

Thermal Radiation Flux Q (Btu/ft^{2}sec) From 1/8-Scale NERVA Exhaust Plume at Selected Locations

Figure 8

RN-S-0168

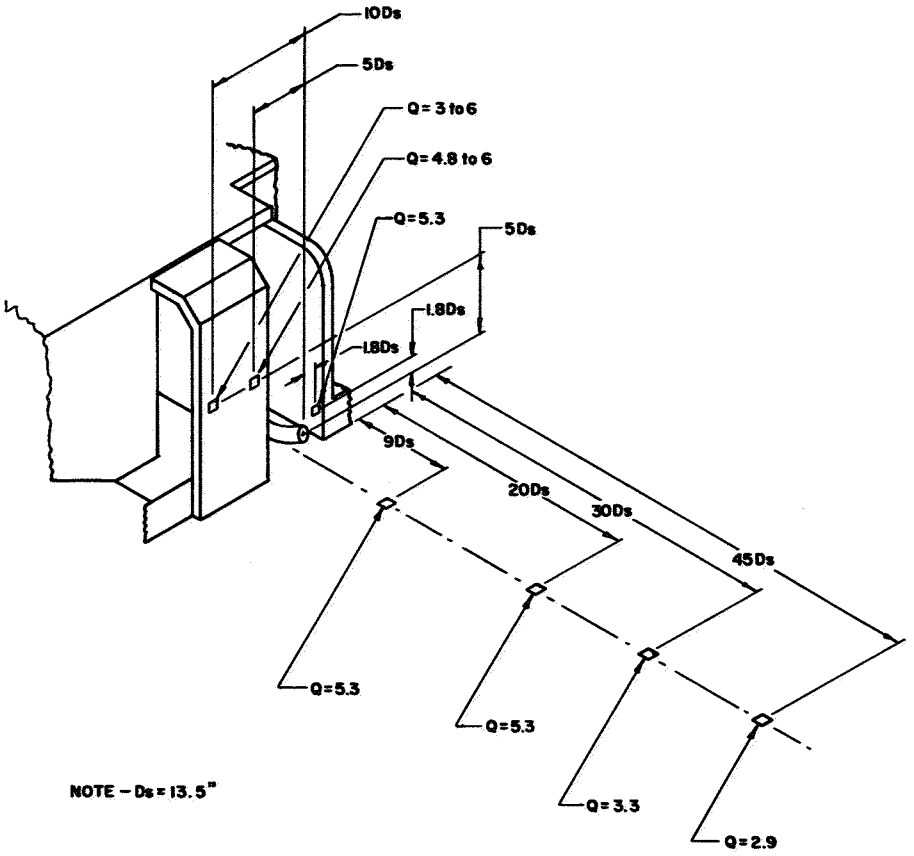

NOTE – Ds = 13.5"

Thermal Radiation Flux Q (Btu/ft^{2}sec) From 1/4-Scale NERVA Exhaust Plume at Selected Locations

Figure 9

NOTES.

1. RADIOMETER HOUSING, INTERIOR SURFACES ARE BLACK
2. SAPPHIRE WINDOW
3. ASYMPTOTIC CALORIMETER, MANUFACTURED & CALIBRATED BY HY-CAL ENGINEERING CO. SANTE FE SPRINGS, CALIFORNIA SENSOR DIAMETER = 1.00 inches

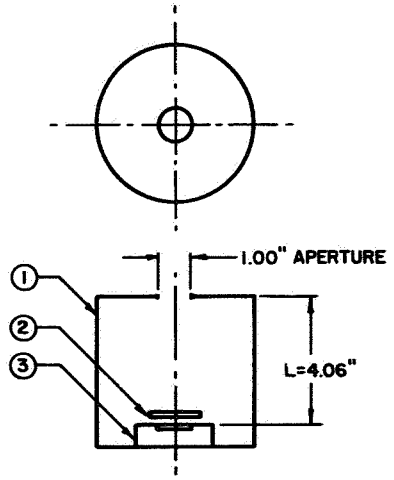

RADIOMETER
(Diagramatic)

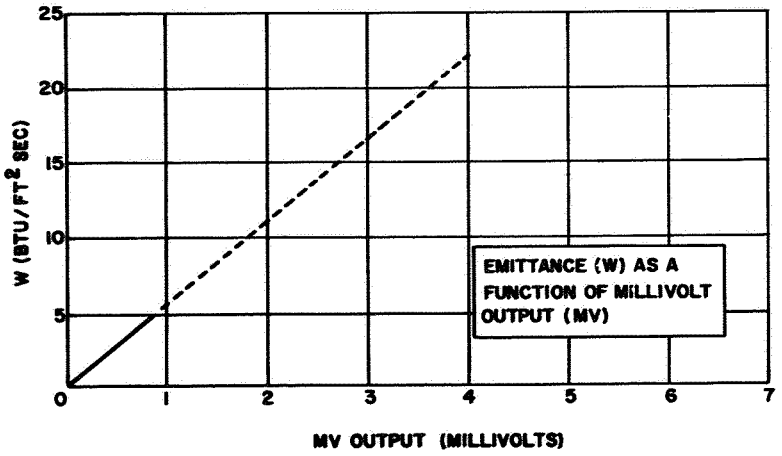

Diagram and Calibration Curve for Radiometer
Used to Measure Exhaust Plume Emittance

Figure 10

RN-S-0168

NOTES.

1.

SYMBOL	FUNCTION
△	H_2 & N_2
○	H_2 ONLY
⊗	1/8 SCALE DATA

2. OPEN SYMBOLS DENOTE APPROXIMATE DESIGN PRIMARY FLOW RATE
3. SOLID SYMBOLS DENOTE APPROXIMATE 1/2 DESIGN PRIMARY FLOW RATE

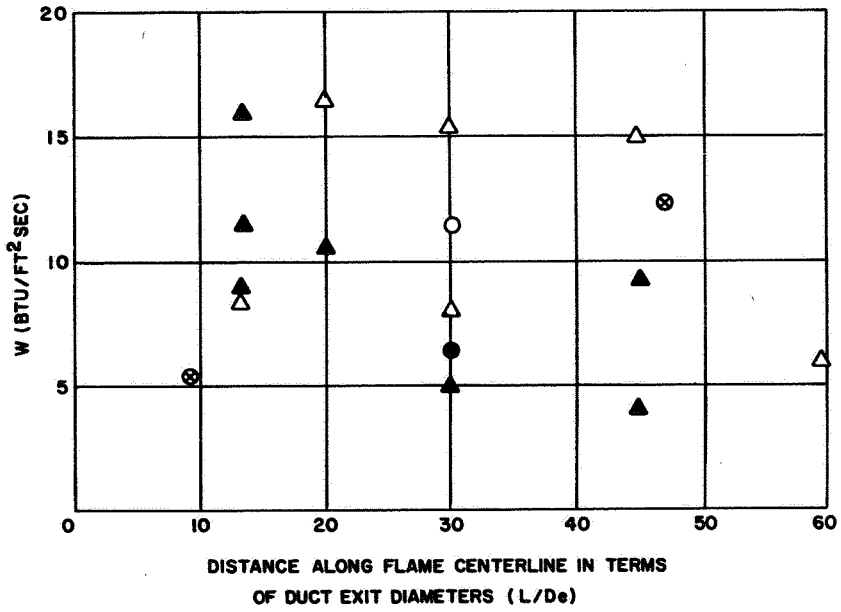

Measured Values of 1/4-Scale Exhaust Plume
Thermal Emittance as a Function of Position
Along Plume Centerline

Figure 11